ISTITUTO NAZIONALE DI FISICA NUCLEARE
Laboratori Nazionali di Frascati

LNF-84/61(P)
11 Ottobre 1984

M. Greco : HARD PROCESSES AT THE $p\bar{p}$ COLLIDER

Lectures given at the "Yukon Advanced Study Institute", Whitehorse, Yukon, August 11-26, 1984

Servizio Documentazione
dei Laboratori Nazionali di Frascati
Cas. Postale 13 - Frascati (Roma)

HARD PROCESSES AT THE $p\bar{p}$ COLLIDER

Mario Greco
INFN - Laboratori Nazionali di Frascati
P.O. Box 13, 00044 Frascati

1. INTRODUCTION

Sp$\bar{p}$S collider results have provided a further and beautiful confirmation that fundamental interactions - electro-weak-strong - are described by gauge theories. In the electro-weak sector the discovery[1,2] of the W and Z bosons, their production properties, the values of their masses and $\sin^2\theta_W$ are in perfect agreement with the theoretical expectations and low energy data. Other questions need to be ansevered now : what is the mechanism for gauge symmetry breaking, do Higgs bosons really exist, are they elementary or composite, are the W and Z gauge bosons and the leptons and quarks elementary, is supersymmetry a property of nature,etc. From many theoretical ideas new phenomena are expected[3] to occur at the 100 GeV-1 TeV energy scale. Indeed new phenomena have been alread observed[4]: appearance of monojets, l + jet + missing $p_\perp$ events, hard jets produced in association with W, Z gauge bosons, etc. However no clear and unique trend emerges from the reported new events and one has to wait for more data from the next Sp$\bar{p}$S collider operation.

In the strong sector on the other hand the new data[4] have provided quite impressive tests of QCD and clear evidence for the non-Abelian structure of the theory. The study of W and Z production and the clear observation of jets with large transverse energy have become quickly an important tool to probe hadron structure, at an energy scale comparable to an e^+e^- storage ring with $\sqrt{s} \sim 100$ GeV.

In the following lectures I will focus on some aspects of QCD at collider energies, concerning W, Z physics and jet phenomena, which have been expected to provide new and decisive tests of the theory in the new energy domain. Additional discussions of the subject, including also tentative interpretations of the new peculiar phenomena, can be found in the recent literature[3,5,6].

Quite generally, testing QCD is in principle more difficult than testing the electroweak theory due to the lack of observing directly quarks and gluons, unlike leptons and gauge bosons. Theoretical predictions often depend explicitly upon phenomenological models of hadronization. Furthermore perturbation theory cannot always be applied and next-to-leading order corrections are sometimes non-negligible. Nevertheles previous tests of QCD, both qualitative (i.e. jets in e^+e^-, large $p_\perp$ phenomena, ...) and quantitative ($R_{e^+e^-}$, scaling violations in deep inelastic scattering, Drell-Yan processes,...- with next-to-leading corrections evaluated -), have given converging evidence in favor of the theory at the scale $Q^2 \sim \sim 10-10^3$ GeV^2.

At the Sp$\bar{\text{p}}$S collider one tests QCD in a new energy domain with sometimes new parton configurations. For example hadron-hadron collisions lead to spectacular effects in jet phenomena with dramatic importance of gluon effects, new quarks flavours are excited, multigluon radiation produces strong effects on the weak bosons production properties, etc. Furthermore the relevant predictions can be deduced unambigously only by the QCD improved parton model.

The outline of this report is as follows. Section 2 discusses jet phenomena in the framework of perturbative QCD. Section 3 reviews vector boson production, with particular emphasis on p_T properties, and related effects in hadron collisions. Finally Section 4 contains our conclusions.

2. JET PHENOMENA

Jets have long been expected[7] to appear as clear evidence for the parton substructure of the hadrons. They have been first observed[8] at the highest ISR energies ($\sqrt{s} \gtrsim 50$ GeV) but have been unambigously produced only at Sp$\bar{\text{p}}$S collider[4,9,10] with a production cross section a few orders of magnitude bigger and p_T up to ~ 100 GeV.

The jet yield is calculated using the improved parton model formula

$$d\sigma\,(a+b \to c+X) = \tag{1}$$
$$= \sum_{ij} \int_0^1 dx_1 dx_2 f_i^{(a)}(x_1,Q^2) f_j^{(b)}(x_2,Q^2)\, d\hat{\sigma}\,(ij \to cX) ,$$

where the sum runs over different types of partons, $d\hat{\sigma}$ is the subprocess differential cross section, and the structure functions are considered to a scale Q^2 of order p_T^2 . The exact appropriate scale ($Q^2 \sim p_T^2$, $p_{T/2}^2$, ...) can be fixed only after computation of next to leading terms.

More generally, it is useful to introduce[11] the concept of differential luminosity of parton-parton collisions at a given c.m. energy $\sqrt{s}$ of the colliding partons :

$$\tau \frac{d\mathscr{L}^{ij}}{d\tau} = \tag{2}$$
$$= \frac{\tau}{(1+\delta_{ij})} \int_\tau^1 \frac{dx}{x} \left[f_i^{(a)}(x) f_j^{(b)}\left(\frac{\tau}{x}\right) + f_j^{(a)}(x) f_i^{(b)}\left(\frac{\tau}{x}\right) \right] ,$$

where $\tau \equiv \hat{s}/s$, with $\sqrt{s}$ the c.m. energy of colliding hadrons a and b. This differential luminosity represents the number of parton-parton collisions with scaled c.m. energies in the interval (τ , $\tau + d\tau$) per hadron-hadron collision. Then for the hadronic reaction (1) one **obtains**, for example,

$$\frac{d\sigma}{d\tau}(ab \to c+X) = \sum_{ij} \tau \left(\frac{d\mathscr{L}^{ij}}{d\tau}\right) \hat{\sigma}(ij \to c) . \tag{3}$$

The parton-parton luminosity measures therefore the relative importance of a given combination of partons for a fixed beam type. Of course the cross section $\hat{\sigma}(\hat{s}) \sim c/\hat{s}$ weights further the contribution of a given subprocess to the hadronic reaction of interest. As an illustration we plot in Figs.1[11] the quantity ($\tau/\hat{s})(d\mathscr{L}/d\tau$), which has dimensions of a cross section as a function of $\sqrt{\hat{s}}$, for total c.m. energies ranging between 2 and 100 TeV. They correspond respectively to the gg, qg and qq contributions in pp collisions, or similarly, gg, $q(\bar{q})g$ and $q\bar{q}$ in $p\bar{p}$ collisions. The luminosity are based upon the parton distribution of ref.11). By direct comparison of Figs.1 it is quite clear the dominance of gluon interactions at $\sqrt{\hat{s}} \lesssim 0.1$ TeV and $\sqrt{s} \sim 1$ TeV. This fact, together with

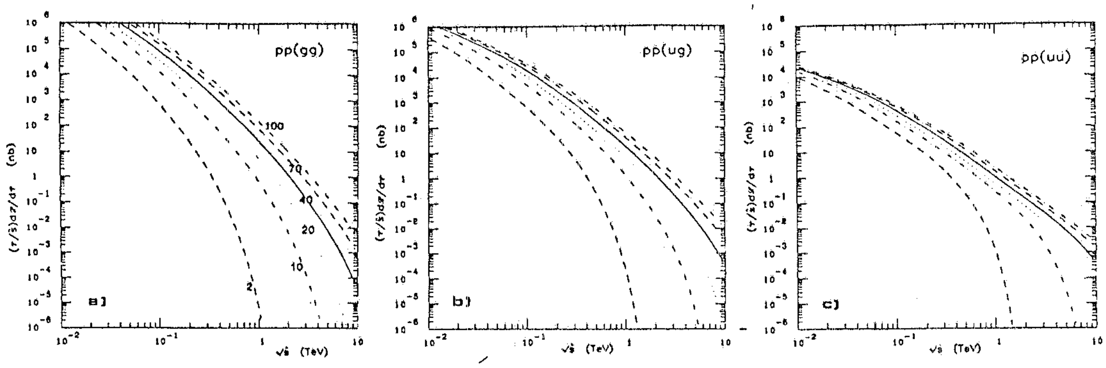

Fig. 1

the large gluon cross sections discussed below, gives to the Sp$\bar{p}$S collider quite a good chance to first reveal the manifestation of the non-Abelian character of the theory.

To lowest order QCD the parton-parton cross sections are given[12)]

$$\frac{d\sigma}{d\hat{t}} = \pi \frac{\alpha_s^2(Q^2)}{\hat{s}^2} \left| A(\hat{s},\hat{t},\hat{u}) \right|^2 , \qquad (4)$$

where $\hat{s},\hat{t},\hat{u}$ are the usual Mandelstam variables and $|A(\hat{s},\hat{t},\hat{u})|^2$ is indicated in Table I for nine different subprocesses, with its numerical value at 90° in the parton parton centre of mass. On the basis of these parton cross sections it is clear that processes involving initial state gluons are largerly favoured also due to colour factors.

Experimentally, events with two clear wide angle jets dominate the background when requiring a sufficiently large amount of transverse energy ($E_T \gtrsim 100$ GeV). Then one has been able to test various predictions of QCD, in spite of the uncertainties associated to the theory, mainly coming from the choice of the scale Q^2, the parametrization of the structure functions and the higher order corrections, as discussed later.

First the jet angular distribution has been found very indicative of vector exchange in parton parton scattering. This is evident from Figs.2 when the UA1 and UA2 results have been shown[13,14)]. In particular, the three almost overlapping lines in Fig. 2a and the area between the two broken curves in Fig. 2b show clearly that the dominant subprocesses behave almost the same, corresponding to the $(\sin \theta^*/2)^4$ behaviour common

Table I - Parton cross-sections : $d\sigma/dt = (\pi\alpha_s^2/s^2)|M|^2$ [averaged (summed) over initial (final colours and spins]. s, t, u refer to the parton processes. F_M is the value of $|M|^2$ at c.m. angle $\theta = 90°$ (s:t:u = 4:-2:-2).

PARTON PROCESS	$\|M\|^2$	F_M
$qq' \to qq'$ $q\bar{q}' \to q\bar{q}'$	$\frac{4}{9}\frac{s^2+u^2}{t^2}$	2.22
$qq \to qq$	$\frac{4}{9}(\frac{s^2+u^2}{t^2}+\frac{s^2+t^2}{u^2}) - \frac{8}{27}\frac{u^2}{st}$	3.26
$q\bar{q} \to q'\bar{q}'$	$\frac{4}{9}\frac{t^2+u^2}{s^2}$	0.22
$q\bar{q} \to q\bar{q}$	$\frac{4}{9}(\frac{s^2+u^2}{t^2}+\frac{t^2+u^2}{s^2}) - \frac{8}{27}\frac{u^2}{st}$	2.59
$q\bar{q} \to gg$	$\frac{32}{27}\frac{u^2+t^2}{ut} - \frac{8}{3}\frac{u^2+t^2}{s^2}$	1.04
$gg \to q\bar{q}$	$\frac{1}{6}\frac{u^2+t^2}{ut} - \frac{3}{8}\frac{u^2+t^2}{s^2}$	0.15
$qg \to qg$	$-\frac{4}{9}\frac{u^2+s^2}{us} + \frac{u^2+s^2}{t^2}$	6.11
$gg \to gg$	$\frac{9}{2}(3 - \frac{ut}{s^2} - \frac{us}{t^2} - \frac{st}{u^2})$	30.4

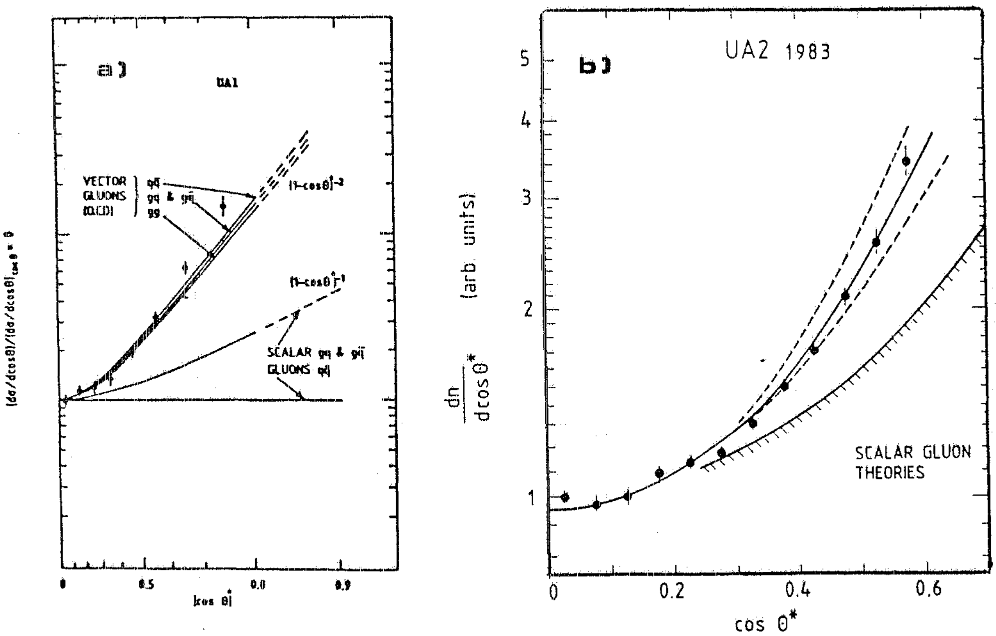

Fig. 2

to all.

Using this almost universal behaviour and the approximate ratios of cross sections $\sigma_{qq}: \sigma_{qg}: \sigma_{gg} \approx 1:(9/4):(9/4)^2$, one can then extract from the data the effective structure function,

$$F(x) = G(x) + \frac{4}{9}\left[q(x) + \bar{q}(x)\right] , \qquad (5)$$

which can be compared with the expectations from low energy neutrino data. This is shown[13,14] in Figs. 3, where it is clear the essential role played by gluons at low x.

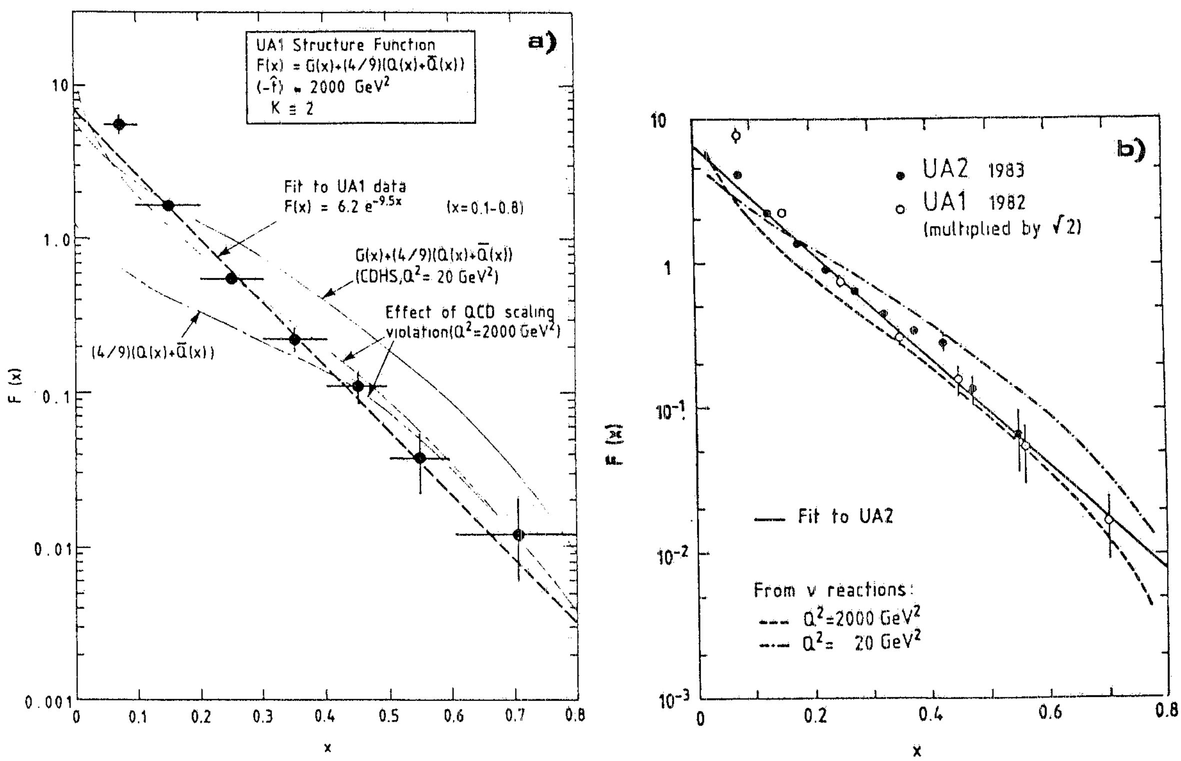

Fig. 3

The inclusive jet yield measured by UA2 is compared in Fig.4 with the absolute QCD prediction of ref.15). The theoretical expectation is reasonably stable against changes of sale in $\alpha_s(Q^2)$ and of the structure functions. The corresponding uncertainty, which is not shown in the figure, is little affecting the shape of the curve and could mainly change the overall scale by a factor 2-3, in particular by effect of higher order corrections (k factors). These are far to be calculated completely, but only partially attempted, as discussed below. The a priori surprising stability of the theoretical prediction in spite of our poor knowledge of the gluon distribution function can be easily understood. In fact, despite possible large differences at low Q^2, various gluon densities become practically identical at the scale relevant for high p_T jets, as illustrated[16] in Fig. 5.

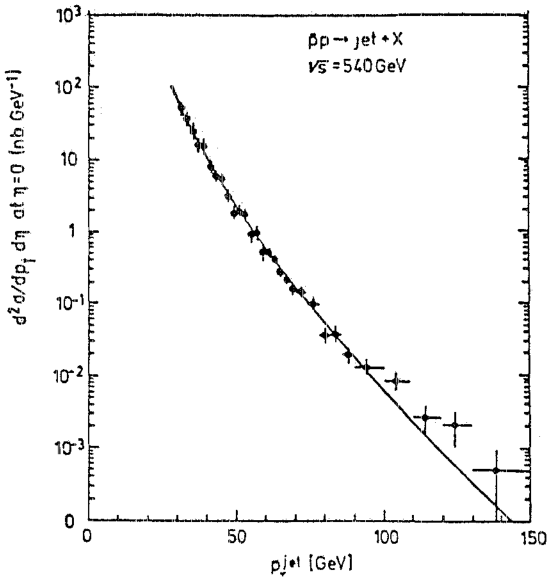

Fig. 4

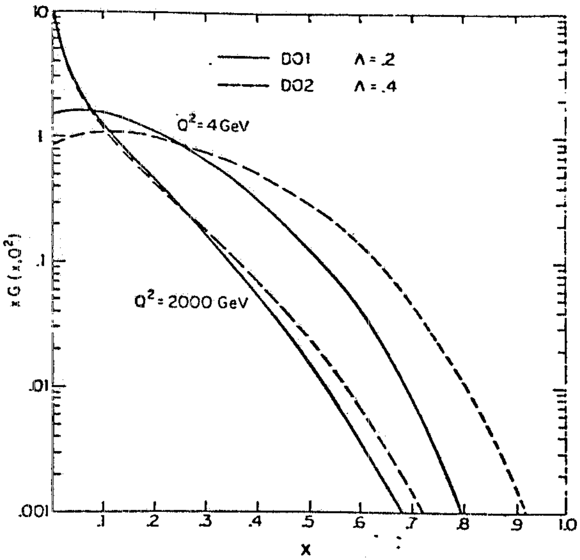

Fig. 5

The effect of removing the gluon vertex from the theory, as an indication of the sensitivity of the result to the non-Abelian coupling, is shown[15] in Fig. 6 under various assumptions. One clearly obtains a

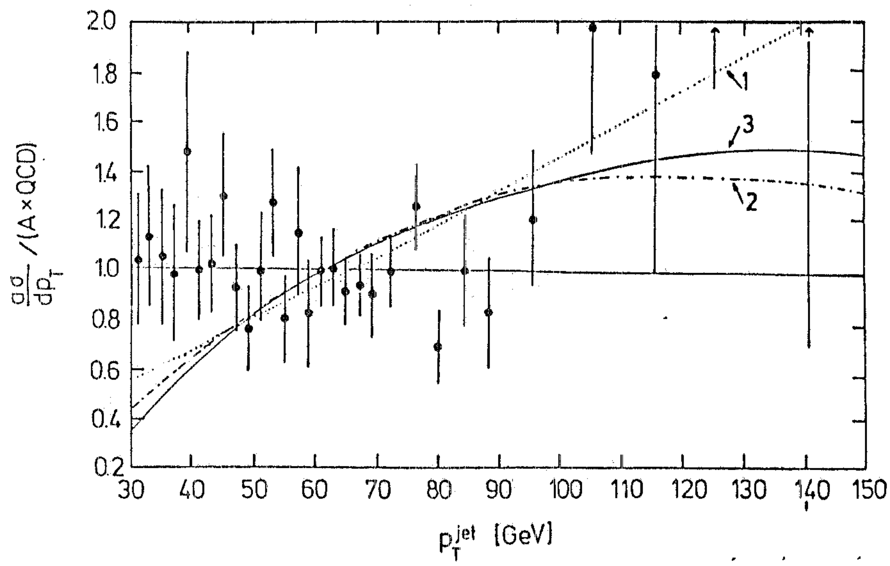

Fig. 6 - Ratios of normalized QCD predictions where the contributions from the three gluon vertex has been removed in elementary parton-parton scattering (1), removed also in the evolution equations (2), and in addition α_s = constant (3). The data are those of Fig. 4.

much worse fit to data.

The effect of the three gluon coupling can be also revealed directly by looking at the transverse momentum unbalance of the two almost back--to-back jets, as the result of bremsstrahlung from the initial gluon legs[17]. The resulting distribution is strongly dependent upon the non-Abelian colour factor C_A (C_A=3), to be contrasted to the case of the weak bosons p_T distribution, which essentially depends on the quark gluon coupling C_F (C_F=4/3). This effect will be discussed in detail later.

We have so far limited our discussion to jet production to order α_s^2. The production of three well separated jets at large p_T clearly corresponds to the $O(\alpha_s^3)$ perturbative description of ($2 \rightarrow 3$) parton subprocesses. The full calculation of such terms has been performed[18] and the results can be cast[19] in a suggestive simple form, which seems to generalize the well known factorization of infrared singularities in the soft limit. It reads (p_i, p_j,... are generic partons)

$$\sigma(p_i+p_j \rightarrow p_k+p_l+g) = |M|^2 I \ , \qquad (6)$$

where $|M|^2$ and I approach the non radiative cross section $|M_o|^2$ and the infrared factor respectively when the momentum k_g of the additive gluon vanishes. Of course those results are only valid away from the regions of soft and collinear singularities. Indeed the complete calculation of $O(\alpha_s^3)$ corrections to the ($2 \rightarrow 2$) subprocesses is still missing because of its complexity, especially in the case of gluon-gluon scattering. Some very special terms of soft origin have been identified[20], similarly to the π^2 term in the Drell-Yan K factor, but the full computation is far from being completed. This lack of information is also at the origin of the ambiguity of the choice of the scale Q^2 in the parton densities and in the running coupling constant. The only suggestion we have, i.e. $Q^2 = p_T^2/2$, comes from the calculation[21] of the reaction $q_i+q_j \rightarrow q_i+q_j+g$. It clearly follows from the above discussion that the perturbative $O(\alpha_s^2)$ results for two jet production cannot be accurate better than a factor of two or so.

An easy test of three jet production is obtained by looking at the acoplanarity distribution of three jet events (p_T-out of the event plan), as shown[22] in Fig. 7. The comparison with experiment is only possible however after using some detailed hadronization model. The agreement with data is quite satisfactory.

Perturbative QCD not only predicts the emergence of jets in hard collisions, but in addition gives well definite predictions for the Q^2 dependence of the parton multiplicity within hard jets. Indeed this problem has been very carefully studied[23] recently and only a systematic treatment of all higher orders beyond the ladder approximation leads to the correct result

$$\langle n(Q^2)\rangle \sim C(\ln \frac{Q^2}{\Lambda^2})^{C_1} \exp(\frac{2C_A}{\pi b} \ln \frac{Q^2}{\Lambda^2})^{1/2} \qquad (7)$$

with $b = (11C_A-2N_f)/12$ and $C_1 \sim 1$. The assumption that the hadronization mechanism does not depend significantly upon Q^2 leads to expect the same Q^2 behaviour for the hadronic multiplicity in the jet. Of course this expectation cannot be naively extended to the total multiplicity observed in $p\bar{p}$ collisions, because additional soft (low p_T) processes might play an important role. With these caveats one can try to compare Sp$\bar{p}$S jets with e^+e^- jets, predominantly gluon and quark jets respectively. The corresponding multiplicities are expected asymptotically to be in the ratio

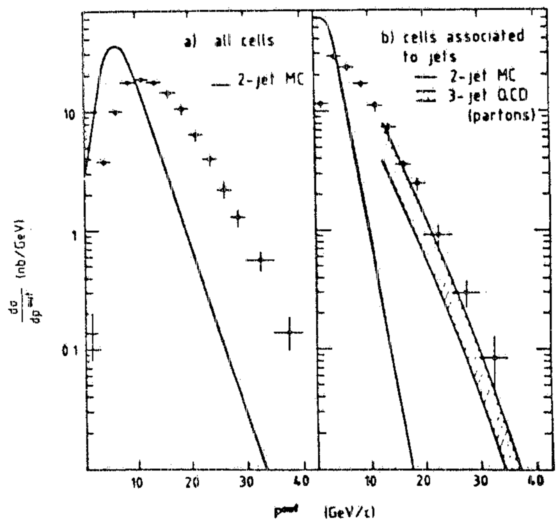

Fig. 7

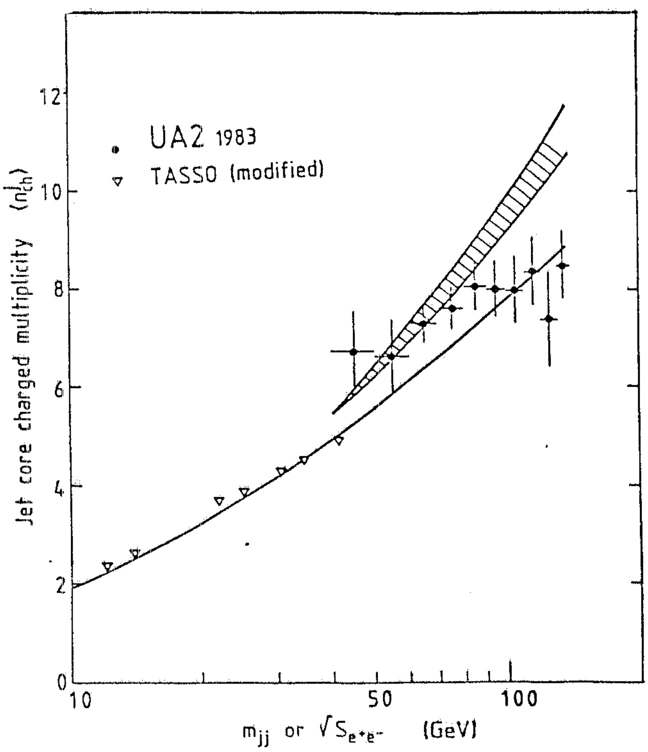

Fig. 8

$C_A/C_F = 9/4$. This task can only be accomplished after using a suitable fragmentation model for quarks and gluons. A recent analysis[24] of UA2 and TASSO data using a QCD Montecarlo[25] seems indeed to suggest a transition from a quark dominated to a gluon dominated distribution, as shown in Fig. 8.

Other observable differences between quark and gluon jets, which have to rely heavily on detailed hadronization models, will not discussed here.

We conclude here our discussion of jet phenomena in the framework of perturbative QCD. Additional results will be given in the next Section, after a general discussion of the theoretical approach to the problem of q_T distribution of Drell-Yan pairs and weak bosons.

3. VECTOR BOSON PRODUCTION AND RELATED PHENOMENA

The production of W and Z bosonss tests the Drell-Yan mechanism of quark annihilation in a completely new energy regime. The total cross section for vector boson production σ and the rapidity differential cross section $d\sigma/dy$ are predicted by the QCD improved parton model[26] as an expansion in the strong coupling constant α_s. The corrections of order α_s to these cross-sections have been calculated and found to be important[27]. They increase the naive parton model prediction by an energy and rapidity dependent factor commonly referred to as the "K-factor". At fixed target energies the $O(\alpha_s)$ corrections are dangerously big and resummation techniques must be invoked[28] in an attempt to control the perturbation series. At collider energies their size is reduced because the coupling constant is smaller and, for the production of weak intermediate bosons, they lead to a correction of about 30%. The total cross-section is therefore more reliably predicted by perturbation theory at these energies with a smaller theoretical error on the overall normalization.

The relevant formulae are given here for the case of Drell-Yan pairs, of Z and W production

$$Q^2 \frac{d\sigma^{\gamma^*}}{dQ^2} = \frac{4\pi\alpha^2}{9S} K \sum_f e_f^2 \int dx_1 dx_2\, \delta(x_1 x_2 - \tau) \left\{ q_f(x_1,Q^2)\bar{q}_f(x_2,Q^2) + (1\leftrightarrow 2) \right\} \tag{8a}$$

$$\sigma^Z = \frac{\pi^2 \alpha}{12\sin^2\theta_W \cos^2\theta_W} \frac{K}{S} \sum_f n_f^Z \cdot$$

$$\cdot \int dx_1 dx_2 \, \delta(x_1 x_2 - \tau) \left\{ q_f(x_1,Q^2)\bar{q}_f(x_2,Q^2) + (1 \leftrightarrow 2) \right\} , \tag{8b}$$

$$\sigma^W = \frac{\pi^2 \alpha}{3\sin^2\theta_W} \frac{K}{S} \int dx_1 dx_2 \, \delta(x_1, x_2 - \tau) \cdot$$

$$\cdot \left\{ u(x_1,Q^2)\bar{d}(x_2,Q^2)\cos^2\theta_C + u(x_1,Q^2)\bar{s}(x_2,Q^2)\sin^2\theta_C + \ldots \right\} , \tag{8c}$$

where $\tau = Q^2/S$ ($Q^2 = M^2$ for the weak bosons), e_f are the quark charges, n_f^Z the coupling of the Z boson to the quarks $n_f^Z = (1-(4/e_f)/\sin^2\theta_W)^2+1$ and K is the K-factor[29]. The other notations are standard. Using the parton luminosities defined in Eq.(2), the weak bosons production cross section can be put in the simple forms

$$\sigma^Z = \frac{G_F \pi}{6\sqrt{2}} K \sum_f n_f^Z \, \tau\left(\frac{d\mathcal{L}}{d\tau}\right)^{q_f\bar{q}_f} ,$$

$$\sigma^W = \frac{G_F \pi \sqrt{2}}{3} K \left[\tau\left(\frac{d\mathcal{L}}{d\tau}\right)^{u\bar{d}} \cos^2\theta_C + \tau\left(\frac{d\mathcal{L}}{d\tau}\right)^{u\bar{s}} \sin^2\theta_C + \ldots \right] \tag{9}$$

where we have made use of $M_Z^2 = M_W^2/\cos^2\theta_W = \pi\alpha/G_F\sqrt{2}\sin^2\theta_W\cos^2\theta_W$. Then in Fig. 9 is shown[30] the departure from the simple parton model results, together with the theoretical uncertainties related to different choices of the structure functions and Λ. Very recent[31] theoretical values for the total production cross sections at $\sqrt{s}$ = 540 GeV are :

$$\sigma^{W^+ + W^-} = (4.2 \begin{smallmatrix} +1.3 \\ -0.6 \end{smallmatrix}) \text{ nb} , \qquad \sigma^Z = (1.3 \begin{smallmatrix} +0.4 \\ -0.2 \end{smallmatrix}) \text{ nb} . \tag{10}$$

Multiplying these numbers by the branching ratios into electrons,

$$B(W^\pm \rightarrow l^\pm \overset{(-)}{\nu}) = 0.089 , \qquad B(Z \rightarrow e^+e^-) = 0.032 , \tag{11}$$

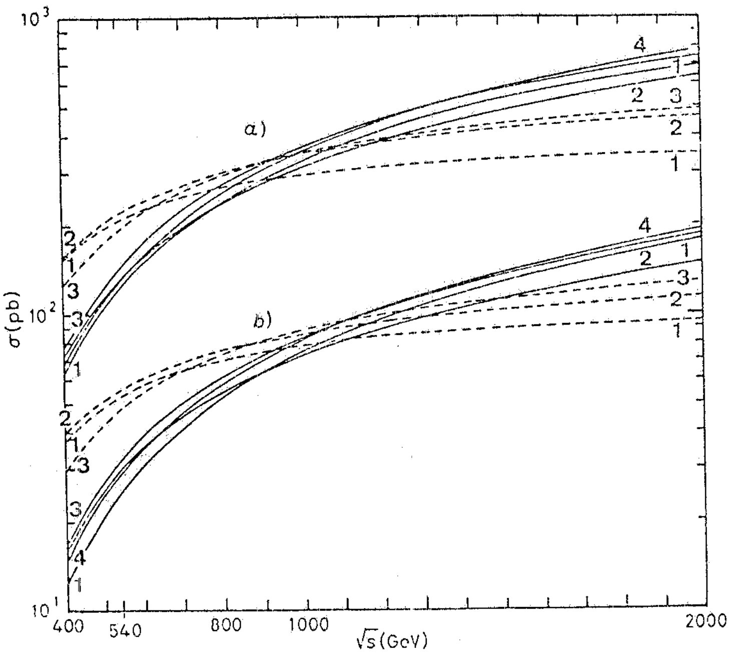

Fig. 9 - $p\bar{p} \to W(\to l\nu)+X$ (a) and $p\bar{p} \to Z(\to ll)+X$ (b) cross sections as a function of $\sqrt{s}$. Dashed lines correspond to Born contributions and solid lines to leading order. The numbers correspond to various parametrizations of the structure functions.

corresponding to $m_t = 40$ GeV and $\alpha_s/\pi = 0.04$ the predictions for the observed decay channels are

$$(\sigma B)_{W^\pm \to e^\pm} = (370 \, ^{+110}_{-60}) \text{ pb} , \quad (\sigma B)_{Z \to e^\pm} = (42 \, ^{+12}_{-6}) \text{ pb} \qquad (12)$$

The corresponding experimental results are[32] :

$$\begin{aligned} &\text{UA1 :} \quad (\sigma B)^{W^\pm} = 530 \pm 80 \pm 90 \text{ pb} , \quad (\sigma B)^{Z^0} = 71 \pm 24 \pm 13 \text{ pb} \\ &\text{UA2 :} \quad (\sigma B)^{W^\pm} = 530 \pm 100 \pm 100 \text{ pb} , \quad (\sigma B)^{Z^0} = 110 \pm 40 ^{+}{-20} \text{ pb} . \end{aligned} \qquad (13)$$

Notice that the ratio of the cross sections (10) is less affected by theoretical errors

$$\frac{\sigma^{W^+ + W^-}}{\sigma^Z} = 3.3 \pm 0.2$$

and is important in order to obtain Γ_W / Γ_Z from experiment.

The prediction of the boson transverse momentum distribution is more subtle, since all order effects need to be taken into account.

Renormalization group improved perturbation theory is valid when the transverse momentum q_T is of the same order as the vector boson mass Q. The large q_T tail of the transverse momentum distribution was one of the early predictions of the QCD improved parton model[33]. As q_T becomes less than Q, such that $\Lambda \ll q_T \ll Q$, a new scale is present in the problem and large terms of order

$$\frac{1}{q_T^2} \alpha_s^n(q_T^2) \ln^m(Q^2/q_T^2) , \qquad (m \leq 2n-1)$$

occur, forcing the consideration of all orders in n. These terms are characteristic of a theory with massless vector gluons. Fortunately, in the leading double logarithmic approximation (DLA: m = 2n-1) these terms can be reliably resummed.This resummation was first attempted by Dokshitzer-Diakonov-Troyan (DDT)[34] and subsequently modified and consolidated[35]. A consistent framework for going beyond the leading double logarithmic approximation has been developed and a complete picture has begun to emerge[36]. The resulting cross sections allow a precise test of the theory in the region $q_T \ll Q$. Of course, at very small q_T ($q_T \sim \Lambda$) non-perturbative effects also become important. For the first generation of Drell-Yan experiments it was difficult to separate clearly the regions $q_T \sim \Lambda$, $\Lambda \ll q_T \ll Q$ and $q_T \sim Q$. At the $p\bar{p}$ collider the observation of the weak bosons q_T distributions gives a unique opportunity to test these theoretical ideas.

In a recent paper[31] the problem of q_T distributions in Drell-Yan processes has be reexamined. The large amount of theoretical information accumulated in recent years has been included in a systematic way. The final expression for the q_T distribution satisfies the following requirements :

(a) At large q_T, we automatically recover the $O(\alpha_s)$ perturbative distribution coming from one-gluon emission, without the ad hoc introduction of matching procedures between hard and soft radiation.

(b) In the region $q_T \ll Q$ the soft gluon resummation is performed at leading double logarithmic accuracy. The role of subleading terms in the summation is also discussed and evaluated.

(c) Only terms corresponding to the emission of soft gluons, for which the exponentiation can be theoretically justified, are resummed.

(d) The integral of the q_T distribution reproduces the known results for the $O(\alpha_s)$ total cross-sections (i.e., including the "K-factor").

(e) The average value of q_T^2 is also identical with the perturbative result at $O(\alpha_s)$.

(f) All quantities are expressed in terms of precisely defined quark distribution functions at a specified scale as for example those determined by the deep inelastic structure function F_2 at the scale Q^2.

The form of the result is,

$$\frac{d\sigma}{dq_T^2 dy} = N \int \frac{d^2b}{(2\pi)^2} \; e^{-\vec{b}q_T} \left[R(b^2,Q^2)\exp S(b^2,Q^2)\right] + Y(q_T^2,Q^2) \qquad (14)$$

where the Sudakov form factor (including only terms which can deduced from an $O(\alpha_s)$ calculation), is

$$S(b^2,Q^2) = \int_0^{A_T^2} \frac{d\mu^2}{\mu^2} \left[J_o(b\,\mu)-1\right] \frac{4}{3} \frac{\alpha_s(\mu)}{2\pi} (2\ln \frac{Q^2}{\mu^2} -3) \; . \qquad (15)$$

The complete $O(\alpha_s)$ expressions for Y and R are given in Ref.(31) and are too complicated to reproduce here. The zeroth order term in R involves the parton distribution functions evaluated at a b-dependent scale

$$R \sim q(x_1^o,B^2)\bar{q}(x_2^o,B^2) + O(\alpha_s) \;, \qquad B^2 \sim 1/b^2$$

with $\tau = M^2/S$, $x^o_{1,2} = \sqrt{\tau}\exp(\pm y)$, and $A_t^2 = \left[(S+Q^2)^2/4S\cosh^2 y - Q^2\right]$ is the kinematical bound of the transverse momentum squared for gluon emission. The function y is completely finite as q_T tends to zero.

The bulk of the q_T distribution, where most of the data have been collected, comes from the soft part of eq.(14). Of course the residual finite terms play a major role for large q_T, say $q_T \gtrsim 30$ GeV where eq. (14) tends to the $O(\alpha_s)$ perturbative result. The so called "leading approximation", where one keeps only the logarithmic term $\ln(Q^2/\mu^2)$ in eq. (15) gives a very poor description of the weak boson distribution and consequently of the decay lepton spectrum, as discussed later.

The numerical consequences of eq.(14) are shown in Fig. 10 with histograms of the UA1 and UA2 W events[32] suitably normalized. The principal uncertainties in eq.(14) are associated with the choice of Λ. This leads to a variation of about 15%, as shown in Fig. 11. The form of the

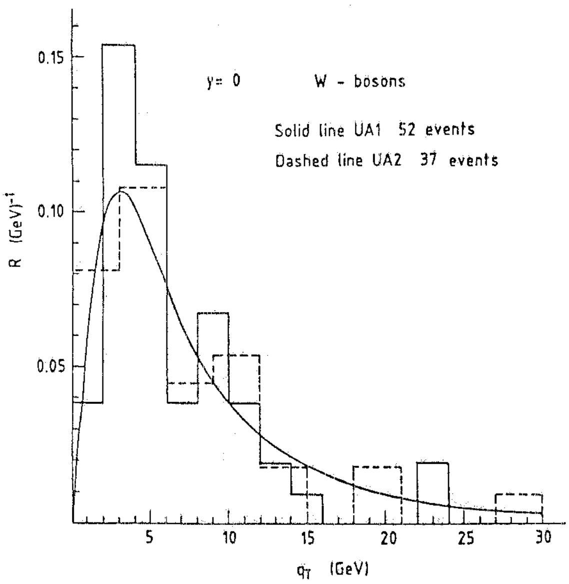

Fig. 10

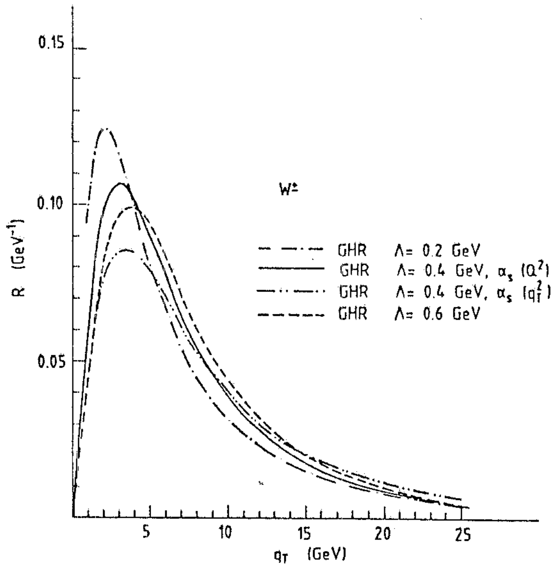

Fig. 11

parton distribution functions leads to a small uncertainty, since quark distributions, well determined in deep inelastic scattering, are most important.

The general structure of eq.(14) has been recently checked[37)] in a recent calculation to order (α_s^2). Writing eq.(15) in a more general form

$$S(b^2,Q^2) = \int \frac{d\mu^2}{\mu^2} \left[J_o(b\mu)-1\right] \left[\ln(\frac{Q^2}{\mu^2})A(\alpha_s)+B(\alpha_s)\right] \qquad (16)$$

with

$$A(\alpha_s) = \sum_i (\frac{\alpha_s}{2\pi})^i A^{(i)} , \qquad B(\alpha_s) = \sum_i (\frac{\alpha_s}{2\pi})^i B^{(i)} ,$$

the new calculation confirms the previous result[38)] for $A^{(2)}$ and also determines $B^{(2)}$. Numerically the additional corrections are of order of $A^{(1)}$ and $B^{(1)}$ and therefore not more important than the uncertainties associated with the choice of the scale Λ.

The p_T distribution of the lepton from the W decay can be obtained[39)] from eq.(14) and is relevant for an accurate determination of the charged boson's mass. In Fig. 12 we show the invariant cross section at a lepton angle $\theta = 90°$. The leading approximation (solid curve), defined above, gives rise to a much broader p_T distribution than the one resulting from the inclusion of subleading terms (dashed curve) corresponding to eq.(14), which is reminescent of what observed for the q_T distribution of the W. The relevant role played by the subleading terms is consistent with the

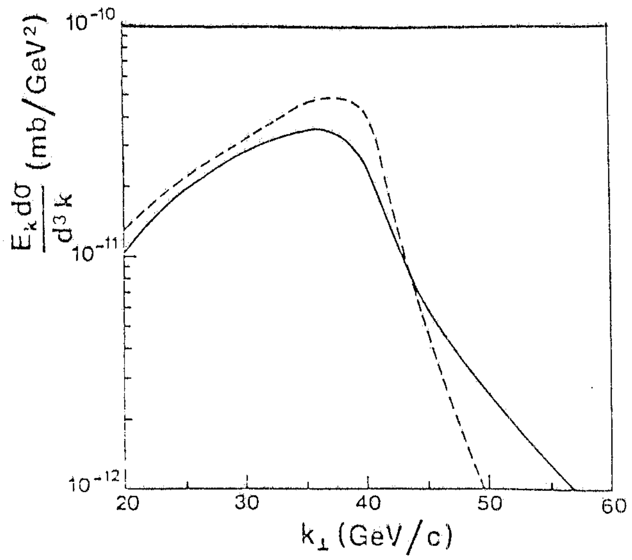

Fig. 12

UA1 data[40], which show no events for $p_\perp$ above 50 GeV.

All the above results have illustrated the idea that W and Z production has quickly become a clear testing ground for perturbative QCD. The theoretical expectations have been generally confirmed. An improved statistics is certainly better suited for further studies, in particular to extract possible new effects from the QCD background.

The mechanism of multigluon bremsstrahlung can also be revealed in purely hadronic processes associated to the hard scattering of the partons. One might envisage two different situations. First one could detect two final almost back-to-back jets, and measure the transverse momentum unbalance. As hinted at the previous Section this allows for a quantitative test of the three gluon coupling[17]. Alternatively, one can look[41,42] at the inclusive distribution of a single variable, e.g. the total transverse energy E_T, well defined experimentally.

More in detail, in the former case, the soft transverse momentum distribution associated to dijet production is given by an expression like eq.(14), where now the Sudakov form factor (15) depends upon the group factors associated to the initial partons-quarks and/or gluons. Due to the dominance of gluon-gluon and quark-gluon scattering at the collider (see Section 2) the resulting p_T^{jj} distribution is quite sensible to non-Abelian effects. This is shown in Fig. 13, where the k_T spectrum obtained by using the Gluck et al.[43] parametrization of the gluon density (full line) is compared to the hypothetical case where gluons would radiate like quarks (dotted line). The theoretical uncertainty associated to the gluon structure function is represented by the dashed line which gives the analogous result for the CDHS[44] parametrization. Experimentally, p_T^{jj} is the vector sum of two large and opposite momenta and is therefore sensitive to instrumental effects. The two components p_η^{ij} (along the bisector of the two jets in the transverse plane) and p_ζ^{ij} (orthogonal to to it and roughly parallel to the two-jet axis) are studied separately, because they are associated with different resolution and systematic effects.

Then the p_{ζ}^{jj}-p_{η}^{jj} distributions are shown[14)] in Fig. 14, compared with the theoretical predictions[17)]. The calculated spectrum (dashed line) is transformed into the histogram when are takes into account detector smearing. Also shown is the expectation (dashed-dotted line) in the hypothetical case where gluons and quarks were to radiate the same way. The close agreement between the expectations and data is a clear evidence for the non-Abelian structure of the theory.

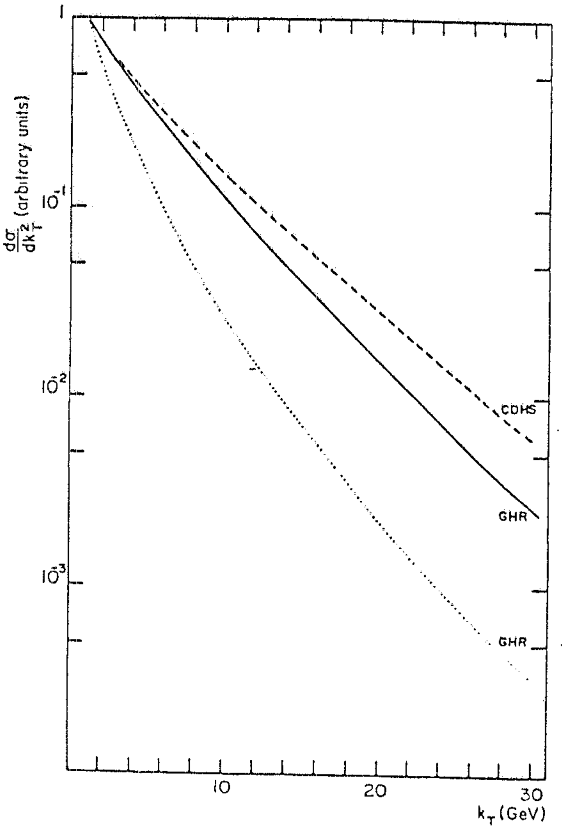

Fig. 13

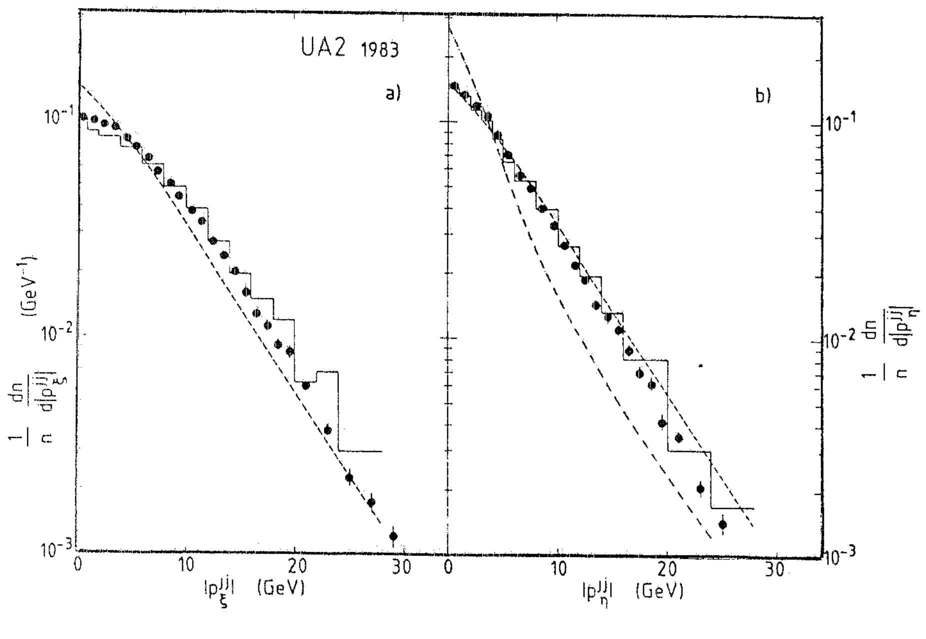

Fig. 14

The mechanism of soft radiation of active partons - mainly quarks (gluons) in W, Z (jet) production - has been suggested[42] to be relevant also in the inclusive production of transverse energy. Indeed it contributes sizeably to the spectrum of $d\sigma/dE_T$, out of the non-perturbative region, and below the region where the two jet system clearly emerges at large angles ($E_T \lesssim \sqrt{s}/2$). This is shown for example in Fig. 15 at ISR energies. The departure of the theoretical curve, which describes only soft effects, from the data[45] is simply related to the actual-experimentally observed-dominance of hard jet production, not included in the calculation.

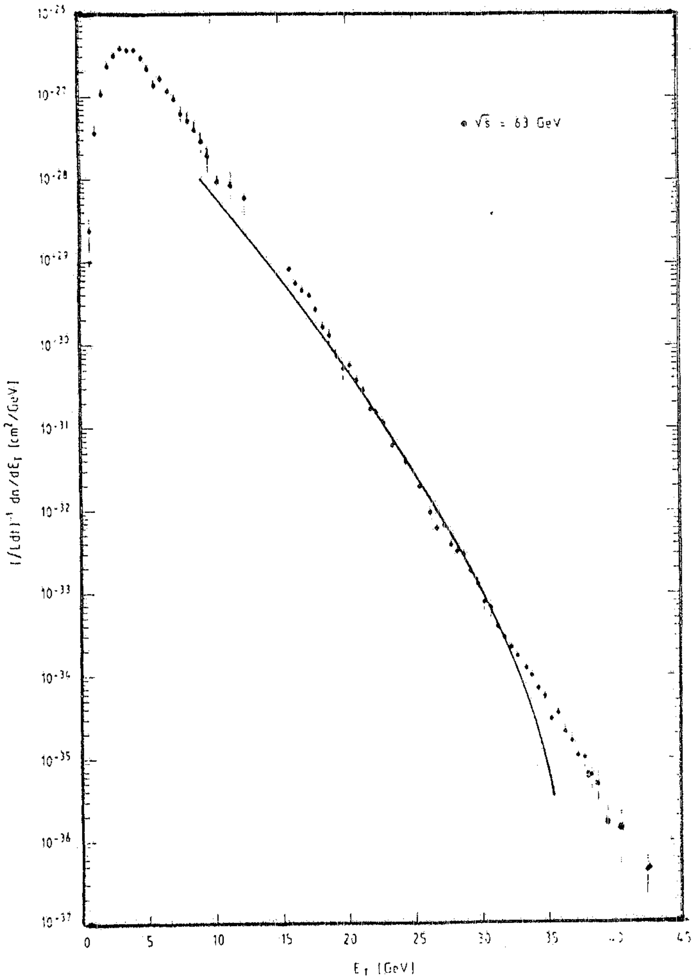

Fig. 15

4. CONCLUSIONS

CERN $Sp\bar{p}S$ collider has become a very reach testing ground for QCD in a new energy domain. Jets have been clearly observed up to $p_T \sim 100$ GeV/c which corresponds to probe the hadron structure at the level of 10^{-16}cm. The production rates and angular distributions have given clear indication in favour of an underlying gauge theory. The production of $W^{\pm}$, Z are also in excellent agreement with the theoretical expections. In particular the theoretical framework of resumming perturbatively soft effects to all orders in α_s has been checked in a general situation of hard parton collision. Quark and gluon jets behave differently, as predicted in a non-Abelian theory. On the theoretical side a full $O(\alpha_s^3)$ calculation of parton-parton scattering, albeit of great complexity, could reduce sensibly the left over uncertainties.

An improved statistical accuracy on the other hand, as expected from the next operation at the $p\bar{p}$ collider, could clearly discriminate the hopefully new physics from the QCD background.

ACKNOWLEDGMENTS

It is a pleasure to thank P.J.O'Donnell, N.Isgur and G.Karl for the invitation to this enjoyable meeting in such a beautiful corner of the world.

REFERENCES

(1) - UA1 Collaboration, Arnison G. et al., Phys. Letters 122B, 103 (1983); 126B, 398 (1983).

(2) - UA2 Collaboration, Banner G. et al., Phys. Letters 126B, 398 (1983); 129B, 130 (1983).

(3) - See for example, Ellis J., Proceedings of the 4th Workshop on $p\bar{p}$ Collider Physics, Bern, 1984.

(4) - UA1 and UA2 Collaborations, Proceedings of the 4th Workshop on $p\bar{p}$ Collider Physics, Bern, 1984.

(5) - Altarelli G., Preprint CERN-TH-3733 (1983); Ellis R.K., Proceedings of the 4th Workshop on $p\bar{p}$ Collider Physics, Bern, 1984.

(6) - Jacob M., Proceedings of the XXII Intern. Conf. on High Energy Physics, Leipzig, 1984.

(7) - See for example Feynman R.P., Photon-Hadron Interactions (Benjamin, 1972).

(8) - Angelis A.L.J. et al., Preprint CERN-EP/83-46 (1983); Akesson T. et al., Preprint CERN-EP/83-71 (1983).

(9) - UA2 Collaboration, Banner M. et al., Phys. Letters 118B, 203 (1982); Bagnaia P. et al., Z.Phys. C20, 117 (1983).

(10) - UA1 Collaboration, Arnison G. et al., Phys. Letters 123B, 115 (1983); 132B, 214, 223 (1983).

(11) - Eichten E. , Inchliffe I,, Lane K. and Quigg C., Fermilab-Pub. 84/17 (1984)

(12) - Combridge B., Kripfganz J. and Ranft J., Phys. Letters 70B, 234 (1977); Cutter R. and Sivers D., Phys. Rev. D16, 679 (1977) and D17, 196 (1978).

(13) - UA1 Collaboration, Arnison G. et al., Phys. Letters 136B, 294 (1984).

(14) - UA2 Collaboration, Bagnaia P. et al., Phys. Letters 144B, 283 (1984).

(15) - Furmanski W. and Kowalski H., DESY Preprint 84-33 (1984).

(16) - Duke D.W. and Owens J.F., Florida State Univ. Preprint FSU/HEP/831115 (1983); see also Ellis R.K., Ref.(5).

(17) - Greco M., Frascati Preprint LNF-84/21 (1984), to appear in Z.Phys. C and Proceedings of the 4th Workshop on $p\bar{p}$ Collider Physics, Bern, 1984.

(18) - Kripfganz J. and Schiller A., Phys. Letters 79B, 317 (1978); Schiller A., J. Phys. G5, 1329 (1979); Maxwell C.J., Nuclear Phys. B149, 61 (1979); Gottschalk T. and Sivers D., Phys. Rev. D21, 102 (1980); Kunszt Z. and Pietarinen E., Nuclear Phys. B164,45 (1980).

(19) - Berends F.A. et al., Phys. Letters 103B, 124 (1981).

(20) - Antoniou N.G. et al., Orsay Preprint LPTHE 83/6 (1983).

(21) - Ellis R.K., Furman M.A., Haber H.E. and Inchliffe I., Nuclear Phys. B173, 397 (1980).

(22) - UA1 Collaboration, Arnison G. et al., Preprint CERN-EP/83-118 (1983).

(23) - Furmanski W. et al., Nuclear Phys. B155, 253 (1979); Bassetto A. et al., Nuclear Phys. B163, 477 (1980); Mueller A., Phys. Letters 104B, 616 (1981).

(24) - UA2 Collaboration, Bagnaia P. et al., Phys. Letters 144B, 291 (1984).

(25) - Marchesini G. and Webber B.R., Nuclear Phys. B238, 1 (1984); Webber B.R., Nuclear Phys. B238, 492 (1984).

(26) - For a review, see Altarelli G., Phys. Rep. 81, 1 (1982).

(27) - Altarelli G., Ellis R.K. and Martinelli G., Nuclear Phys. B157, 461 (1979); Kubar-Andrè and Paige F.E., Phys. Rev. D19, 221 (1979).

(28) - Parisi G., Phys. Letters 90B, 295 (1980); Curci G. and Greco M., Phys. Letters 92B, 175 (1980).

(29) - For a review, see Stirling W.J., Proceedings of the Drell-Yan Workshop, Fermilab (1982), p. 131.

(30) - Chiappetta P. and Perrottet M., Nuovo Cimento 81A, 727 (1984).

(31) - Altarelli G., Ellis R.K., Greco M. and Martinelli G., Preprint CERN-TH-3851 (1984), to appear in Nuclear Phys.

(32) - UA1 Collaboration, presented by Rubbia C., Proceedings of the 4th $p\bar{p}$ Workshop, Bern, 1984; UA2 Collaboration, presented by Schacker J., Proceedings of the 4th $p\bar{p}$ Workshop, Bern, 1984.

(33) - Altarelli G., Parisi G. and Petronzio R., Phys. Letters 76B, 351, 356 (1978); Fritzsch H. and Minkowski P., Phys. Letters 74B, 384 (1978); Kajantie K. and Raitio R., Nuclear Phys. B139, 72 (1978); Halzen F. and Scott P.M., Phys. Rev. D18, 3378 (1978); See also, Aurenche P. and Lindfors J., Nuclear Phys. B185, 274 (1981).

(34) - Dokshitzer Yu.L., Dyakonov D.I. and Troyan S.I., Phys. Letters 78B, 290 (1978); Phys. Rep. 58, 269 (1980).

(35) - Parisi G. and Petronzio R., Nuclear Phys. B154, 427 (1979); Curci G., Greco M. and Srivastava Y., Phys. Rev. Letters 43, 434 (1979); Nuclear Phys. B159, 451 (1979).

(36) - Lo C.Y. and Sullivan J.D., Phys. Letters 86B, 327 (1979); Bassetto A., Ciafaloni M. and Marchesini G., Phys. Letters 86B, 366 (1979); Ellis S.D. and Stirling W.J., Phys. Rev. D23, 214 (1981); Jones H. F. and Wyndham J., Nuclear Phys. B176, 466 (1980); Rakow P.E.L. and Webber B.R., Nuclear Phys. B187, 254 (1981); Ellis S.D., Fleishon N. and Stirling W.J., Phys. Rev. D24, 1386 (1981); Collins J. C. and Soper D.E., Nuclear Phys. B193, 381 (1981); B194,445 (1982); B197, 446 (1982); Chiappetta P. and Greco M., Phys. Letters 106B, 219 (1981); Nuclear Phys. B199, 77 (1982); B221, 269 (1983); Pennington M., Nuclear Phys. B204, 189 (1982); Kodaira J. and Trentadue L., Phys. Letters 112B, 66 (1982); 123B, 335 (1983).

(37) - Davies C.T.H. and Stirling W.J., Preprint CERN-TH.3853 (1984).

(38) - Kodaira J. and Trentadue L., Phys. Letters 112B, 66 (1982); 123B, 335 (1983).

(39) - Chiappetta P., Greco M. and Soffer J., Frascati Preprint LNF-84/14 (1984), to appear in Z.Phys. C.

(40) - UA1 Collaboration, Arnison G. et al., Phys. Letters 129B, 273 (1983).

(41) - Greco M., Phys. Letters 121B, 360 (1983), and Proceedings of the XVII Rencontre de Moriond, ed. by J.Tran Thanh Van (1982); Davies C.T.H. and Webber B.R., Preprint CERN-TH.3628 (1983).

(42) - Greco M., Frascati Preprint LNF-83/51 (1983), to appear on Nuclear Phys.

(43) - Gluck M., Hoffman E. and Reya E., Z.Phys. C13, 119 (1982).

(44) - Adranovicz H. et al., Z. Phys. C12, 289 (1982)

(45) - Akesson T. et al., Ref.(7).